Journal of Alloys and Compounds 480 (2009) 397–402

Contents lists available at ScienceDirect

Journal of Alloys and Compounds

journal homepage: www.elsevier.com/locate/jallcom

Phase equilibria and chemical vapor transport in the system Mo–Ta–As

Peter Raffelstetter[a,b], Klaus W. Richter[a,*]

[a] Department of Inorganic Chemistry/Material Chemistry, University of Vienna, Währinger Straße 42, 1090 Wien, Austria
[b] CEST, Centre of Electrochemical Surface Technology, Viktor-Kaplan-Straße 2, 2700 Wiener Neustadt, Austria

ARTICLE INFO

Article history:
Received 30 January 2009
Accepted 13 February 2009
Available online 26 February 2009

Keywords:
Mo–Ta–As system
Phase diagram
Chemical vapor transport
Crystal structure

ABSTRACT

The phase diagram Mo–Ta–As was studied in two partial isothermal sections at 1050 °C (in the As-rich corner) and at 1400 °C (As-poor alloys) using powder X-ray diffraction and electron probe microanalysis. A complete solid solution was found to exist between isostructural Mo_5As_4 and Ta_5As_4 and the ternary solubility of Mo in Ta_3As at 1400 °C was determined. A ternary phase $Mo_xTa_{1-x}As$ with MnP-type structure was found to exist in the As-rich part of the system. Lattice parameters were investigated as a function of composition for $(Mo,Ta)_5As_4$ and for $Mo_xTa_{1-x}As$. Additional experiments of chemical vapor transport (CVT) from 1000 °C to 900 °C using different ternary source compositions and I_2 and Br_2 ($PtBr_2$) as transport agents were performed. Only Ta compounds were found in the sink and no ternary transport was observed.

1. Introduction

This investigation is part of an ongoing research project on phase equilibria, crystal structures and partial ordering in ternary systems composed of two early transition metals in combination with arsenic, germanium or gallium. We report our study of phase equilibria and chemical vapor transport (CVT) in the system Mo–Ta–As, which has not been investigated up to now.

The bordering binary systems have been investigated in detail. In the system Mo–As, Taylor et al. [1] and Jensen et al. [2] identified three compounds, which they found to be the only intermediate phases. The crystal structures of these compounds were determined by single crystal diffraction: Mo_5As_4 [3], Mo_2As_3 [4] and $MoAs_2$ [5]. Boller and Nowotny [6] reported the existence of MoAs, which could not be confirmed by other authors [1,2]. Later, a study conducted by Guerin et al. [7] showed that "MoAs" is actually stabilized by adding other transition metal arsenides MAs (M = Fe, Cr, V, Mn, Ti). The phase $Mo_xM_{1-x}As$ was found to be stable for up to 90–95 at.% of Mo, but not beyond that. In addition, Brown [5] mentioned $MoAs_5$, but the existence of this compound was not confirmed by other authors. A calculated phase diagram of the Mo–As system was published by Brewer and Lamoreaux [8]. Information on crystal structures of binary Mo–As compounds is given in Table 1.

Chemical vapor transport in the system Mo–As was investigated in a comprehensive study by Murray et al. [9]. They succeeded in transporting Mo_5As_4, Mo_2As_3 and $MoAs_2$ using bromine as transport agent in quartz tubes. $MoAs_2$ was as well transported using chlorine. Iodine was found to be inferior as transport agent relative to the halogens just referred to. All transport reactions were of endothermic type, i.e., the transport occurred towards lower temperatures.

In the system Ta–As, five intermediate phases are established. First research in this system focused on the arsenic-rich compounds. Furuseth et al. [10,11] found that $TaAs_2$ is of the $NbAs_2$ structure type having the space group $C2$. Later on, Ling and Belin [12] re-investigated the structure by single crystal diffraction and assigned space group $C2/m$ to $TaAs_2$ and to its structure type $NbAs_2$ respectively. Calvert [13] reviewed several phases with reported $NbAs_2$-type structure and concluded that for all of them $C2/m$ is the appropriate space group. Thus, the correct type structure for these compounds is $OsGe_2$ which was solved earlier in $C2/m$. This also holds for $MoAs_2$, which was reported in $C2$ only. TaAs has been reported by Furuseth et al. [10] and Murray et al. [14]. The metal-rich phases Ta_2As and Ta_5As_4 were prepared for the first time by Rundqvist et al. [15] and the most Ta-rich phase, Ta_3As, by Ganglberger et al. [16]. Wang et al. [17] obtained single crystals of Ta_3As by CVT in tantalum crucibles and were thus able to characterize the new Ta_3As structure type. Structural information on binary Ta–As phases is compiled in Table 1.

In the course of a re-investigation of the metal-rich Ta–As system, Murray et al. [14] used halide vapor transport with the objective of obtaining single crystals for structure determination and refinement. They obtained single crystals of TaAs using the latter compound as source and iodine as transport agent in the down-gradient mode, whereas experiments with chlorine and bromine yielded a $TaAs_2$ at the sink. Ta_2As was transported with iodine to the cooler end of the tube; no other transport agent was tested for this compound. Unlike Ta_2As and TaAs, Ta_3As could not be

* Corresponding author. Tel.: +43 1 4277 52910; fax: +43 1 4277 9529.
E-mail address: klaus.richter@univie.ac.at (K.W. Richter).

0925-8388/$ – see front matter © 2009 Elsevier B.V. All rights reserved.
doi:10.1016/j.jallcom.2009.02.046

Table 1
Crystal structures of binary intermediate phases reported in the systems Mo–As and Ta–As.

Phase	Structure type	Pearson symbol, space group	Lattice parameter/Å	Reference
Mo_5As_4	Ti_5Te_4	*tI*18, *I*4/*m*	*a* = 9.6005(6), *c* = 3.2781(4)	[3]
MoAs[a]	MnP	*oP*8, *Pnma*	*a* = 5.989, *b* = 3.368, *c* = 6.417	[6]
Mo_2As_3	Mo_2As_3	*mC*20, *C*2/*m*	*a* = 13.361(1), *b* = 3.2337(3), *c* = 9.6385(5), β = 124.57(4)°	[4]
$MoAs_2$[b]	$NbAs_2$	*mC*12, *C*2	*a* = 9.067(2), *b* = 3.300(1), *c* = 7.718(2), β = 119.35(3)°	[5]
$MoAs_5$[c]	FeS_2	*oP*6, *Pnnm*	*a* = 5.299(2), *b* = 5.983(2), *c* = 2.885(1)	[5]
Ta_3As	Ta_3As	*mC*64, *C*2/*c*	*a* = 14.6773(6), *b* = 5.0954(2), *c* = 14.5505(4), β = 90.572(3)°	[17]
Ta_2As	Ta_2P	*oP*36, *Pnnm*	a = 14.7680(11), *b* = 11.8373(9), *c* = 3.4696(4)	[15]
Ta_5As_4	Ti_5Te_4	*tI*18, *I*4/*m*	*a* = 9.8038(8), *c* = 3.4344(9)	[15]
TaAs	NbAs	*tI*8, $I4_1md$	*a* = 3.4375(1), *c* = 11.6469(3)	[14]
$TaAs_2$	$NbAs_2$	*mC*12, *C*2	*a* = 9.3385, *b* = 3.3851, *c* = 7.7568, β = 119.70°	[10]
	$GeOs_2$	*mC*12, *C*2/*m*	*a* = 9.331(2), *b* = 3.383(2), *c* = 7.752(2), β = 119.71(2)°	[12]

[a] Stabilized by impurity metals.
[b] Presumably $GeOs_2$ type.
[c] Not confirmed by other authors.

transported in quartz tubes, because the tubes decomposed forming Ta_2Si and β-Ta_2O_5. As mentioned in the paragraph before, the authors had to use tantalum crucibles to succeed in preparing single crystals of this phase.

The two transition metals Mo and Ta (both with W-type structure) show unlimited solid solubility and no compound formation. Mo can be transported with bromine [9] and Ta with bromine [18] and iodine [19], all with exothermic transport reactions.

Given the close chemical relation and the solid solubility of Mo and Ta, the formation of extended substitutional solid solutions is to be expected in the ternary system Mo–Ta–As and it was our aim to investigate the extension of these solid solutions as well as to search for possible new ternary compounds. As successful CVT experiments were reported for Mo–As as well as for Ta–As it was also decided to investigate the possibility of CVT in the ternary system Mo–Ta–As.

2. Experimental

All samples were prepared from molybdenum powder (100 mesh, 99.95%, Alfa Aesar) tantalum powder (100 mesh, 99.98%, Alfa Aesar), and arsenic lump (99.9999%, Johnson Matthey). Twelve samples representative for the arsenic-rich part of the phase diagram were prepared by the following procedure. The proper amounts of the pure elements were weighted, sealed into evacuated quartz glass ampoules and annealed at 1050 °C for 4 weeks in total. The annealing was interrupted weekly in order to grind the samples for a better homogenization and they were quenched when finally taking them out of the furnace. The nominal sample compositions are listed in Table 2 together with experimental results.

Six additional samples were prepared to investigate the metal-rich part of the system at a higher annealing temperature. After weighting the elements, the powder mixtures were annealed in evacuated quartz glass ampoules at 1050 °C for 1 week. The pre-reacted powders were then pressed into pellets and molten twice in the arc furnace. Arc melting was performed on a water-cooled copper plate in inert argon atmosphere. Zirconium was used as a getter material. Subsequently, the samples were put into tantalum crucibles, which were welded in the arc furnace at 0.5 bar argon atmosphere and annealed at 1400 °C for 3 days. The samples were quenched

Table 2
Nominal sample compositions and results of powder XRD for arsenic-rich samples.

Sample #	Nominal sample composition at.% Mo/at.% Ta/at.% As	Phases detected by XRD	Lattice parameter/Å
1	50.1/0/49.9	$(Mo,Ta)_5As_4$	*a* = 9.5991(1), *c* = 3.2769(1)
		Mo_2As_3	*a* = 13.3708(1), *b* = 3.2346(1), *c* = 9.6437(1), β = 124.60(1)°
2	40.0/10.0/50.0	$Mo_xTa_{1-x}As$	*a* = 6.0175(1), *b* = 3.3969(1), *c* = 6.4236(1)
		$(Mo,Ta)As_2$	Traces
3	30.1/20.1/49.8	$Mo_xTa_{1-x}As$	*a* = 6.0556(1), *b* = 3.4289(1), *c* = 6.4385(1)
		TaAs	Traces
		$(Mo,Ta)As_2$	Traces
4	25.1/25.0/49.9	$Mo_xTa_{1-x}As$	*a* = 6.0737(1), *b* = 3.4402(1), *c* = 6.4456(1)
		TaAs	Traces
5	20.1/30.1/49.8	$Mo_xTa_{1-x}As$	*a* = 6.0789(1), *b* = 3.4423(1), *c* = 6.4477(1)
		TaAs	*a* = 3.4366(1), *c* = 11.6441(1)
6	10.1/40.0/49.9	TaAs	*a* = 3.4365(1), *c* = 11.6444(1)
		$Mo_xTa_{1-x}As$	*a* = 6.0849(1), *b* = 3.4452(1), *c* = 6.4502(1)
		$(Mo,Ta)As_2$	Traces
7	0/50.1/49.9	TaAs	*a* = 3.4365(1), *c* = 11.6420(1)
8	44.5/11.2/44.3	$(Mo,Ta)_5As_4$	*a* = 9.6497(1), *c* = 3.2959(1)
		$Mo_xTa_{1-x}As$	Traces
9	33.4/22.3/44.3	$(Mo,Ta)_5As_4$	*a* = 9.6749(1), *c* = 3.3355(1)
		TaAs	Traces
10	27.5/27.5/45.0	$(Mo,Ta)_5As_4$	*a* = 9.6799(1), *c* = 3.3494(1)
		TaAs	Traces
		$Mo_xTa_{1-x}As$	Traces
11	22.4/33.3/44.2	$(Mo,Ta)_5As_4$	*a* = 9.6875, *c* = 3.3775(1)
		TaAs	Traces
12	11.4/44.5/44.1	$(Mo,Ta)_5As_4$	*a* = 9.7142(1), *c* = 3.4156(1)
		TaAs	Traces

Table 3
Phase compositions of the metal-rich samples determined by EPMA.

Sample #	Nominal sample composition at.% Mo/at.% Ta/at.% As	Phase compositions determined by EPMA		
		$(Mo,Ta)_5As_4$ at.% Mo/at.% Ta/at.% As	$Mo_xTa_{3-x}As$ at.% Mo/at.% Ta/at.% As	(Mo,Ta) at.% Mo/at.% Ta/at.% As
13	62.7/18.1/19.2	–[a]	–	82.0/17.4/0.6
14	35.3/35.3/29.4	18.8/37.0/44.2	33.4/42.8/23.8	67.0/31.7/1.3
15	15.5/53.5/31.0	11.6/43.8/44.6	22.2/53.1/24.7	–
16	63.2/21.1/15.7	36.5/19.9/43.6	–	77.7/20.9/1.4
17	42.5/42.5/15.0	–	23.3/52.1/24.6	57.8/39.1/3.1
18	20.6/61.8/17.6	–	5.7/70.1/24.2	28.2/70.0/1.8

[a] Equilibrium composition not measured due to the fine microstructure of the sample.

when taking them out of the furnace. Due to the high vapor pressure of arsenic a loss of this element occurred during melting in the arc furnace and during annealing in tantalum crucibles. The samples were weighted again after their preparation and the decrease of mass is assumed to stem solely from evaporation of arsenic. Thus, for all metal-rich samples the nominal composition is defined as the composition calculated by subtracting the mass loss from the weighted mass of arsenic. Table 3 lists the nominal compositions of these samples together with experimental results.

After crushing the metal-rich samples, a piece of each was embedded into a matrix of resin and copper powder. The surfaces of these were ground and polished in order to perform optical microscopy as well as electron probe microanalysis (EPMA). Investigations by optical microscopy were carried out using a Zeiss Axiotech 100 microscope equipped for operation under polarised light. EPMA measurements were performed with a Cameca SX 100 electron probe using wavelength dispersive spectroscopy (WDS), which was operated at 20 kV and 20 nA. Pure molybdenum, tantalum and gallium arsenide served as standard materials, and conventional ZAF correction was applied to calculate the final compositions.

All samples were investigated by powder X-ray diffraction (XRD). For this purpose, a diffractometer in Bragg–Brentano geometry (Bruker D8 Discover, Cu Kα radiation) was used and the X-ray patterns were refined using the Topas software [20]. While the preparation of powders for XRD was done with a mortar in case of the arsenic-rich samples, a ball mill had to be used to grind the metal-rich samples and stress annealing of these powders for 2 min at 1050 °C was performed after ball milling.

CVT experiments were carried out in quartz glass tubes with an outer diameter of 20 mm and 1.8 mm wall thickness. To remove adsorbed water, the tubes were heated under dynamic vacuum just below their softening point. I_2 and Br_2 (in form of $PtBr_2$, 98%, Sigma–Aldrich) and were used as transport agents. The quartz glass tubes were loaded with the powdered samples and the transport agents in inert argon atmosphere and subsequently evacuated and sealed to a final length of 120 mm. A two-zone furnace was used to establish a temperature gradient with 1000 °C at the source and 900 °C at the sink for all CVT experiments.

Single crystals obtained by vapor transport were analyzed using a Siemens Kristalloflex 710 four circle diffractometer with monochromatic Mo Kα radiation.

3. Results and discussion

3.1. The arsenic-rich part of the Mo–Ta–As system

The phase equilibria found by XRD in the arsenic-rich part of the phase diagram at 1050 °C are listed in Table 2. The samples were prepared along two sections at roughly 50 at.% and 44.4 at.% As, respectively.

In agreement with [7], "MoAs" was not found in the binary system Mo–As (sample #1), but a phase with MnP-type structure was found in all ternary samples with 50 at.% As (samples #2–6), clearly indicating that the MnP-type structure can be stabilized by the addition of Ta. The respective ternary phase is designated $Mo_xTa_{1-x}As$ in Table 2. While the samples #2–4 (10–25 at.% Ta) are essentially pure $Mo_xTa_{1-x}As$ with only traces of impurity phases present, samples #5 and 6 (30 at.% and 40 at.% Ta) show the presence of $Mo_xTa_{1-x}As$ in equilibrium with TaAs indicating the existence of the corresponding two-phase field in this composition area. Plotting the lattice parameters of $Mo_xTa_{1-x}As$ versus composition (Fig. 1) confirms these findings and allows determining the solubility limits of that $Mo_xTa_{1-x}As$. The solubility on the molybdenum-rich side obviously lies between 0 at.% and 10 at.% Ta, but cannot be determined precisely from this data. The solubility limit on the tantalum-rich side is identified from the almost linear variation of the orthorhombic lattice parameters with the composition. The extrapolation (intersection of the straight lines in Fig. 1) points to a solubility limit of 27 ± 2 at.% Ta. In the case of TaAs, the lattice parameters in the binary (sample #7) do not deviate significantly from the parameters observed in equilibrium with $Mo_xTa_{1-x}As$ (samples #5 and 6), indicating a negligible ternary solubility in this compound.

In all samples having 44.4 at.% As, a Ti_5Te_4-type solid solution $(Mo,Ta)_5As_4$ was found. It is thus concluded that the binary phases Mo_5As_4 and Ta_5As_4 (both of Ti_5Te_4-type structure) form an unlimited solid solution. The variation of the lattice parameters with the composition as given in Fig. 2 shows a smooth but significantly non-linear behaviour. The cell volumes shown in Fig. 3, however, vary in an almost linear manner, consistent with Mo/Ta substitution.

Based on our experimental data, a partial isothermal section of the As-rich part of the ternary Mo–Ta–As system at 1050 °C is given in Fig. 4. Although no samples in the section at 33.3 at.% As were prepared in the present study, a complete solid solution between isostructural $MoAs_2$ and $TaAs_2$ is to be expected and the isothermal section is drawn accordingly.

3.2. The metal-rich part of the Mo–Ta–As system

XRD patterns obtained from the metal-rich samples annealed at 1400 °C showed a significant broadening of peaks, which is most likely due to inhomogenities of the samples. The XRD patterns could be used to identify the phases present in the samples, but the

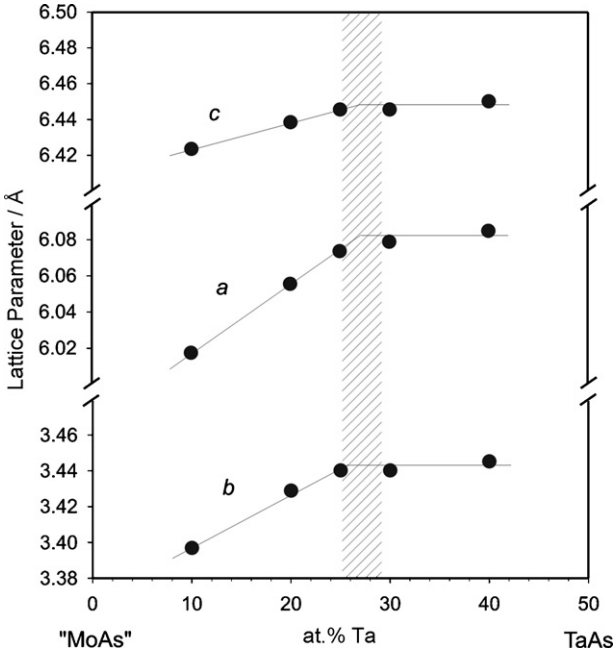

Fig. 1. Lattice parameters of $Mo_xTa_{1-x}As$ (MnP-type structure) versus nominal sample composition.

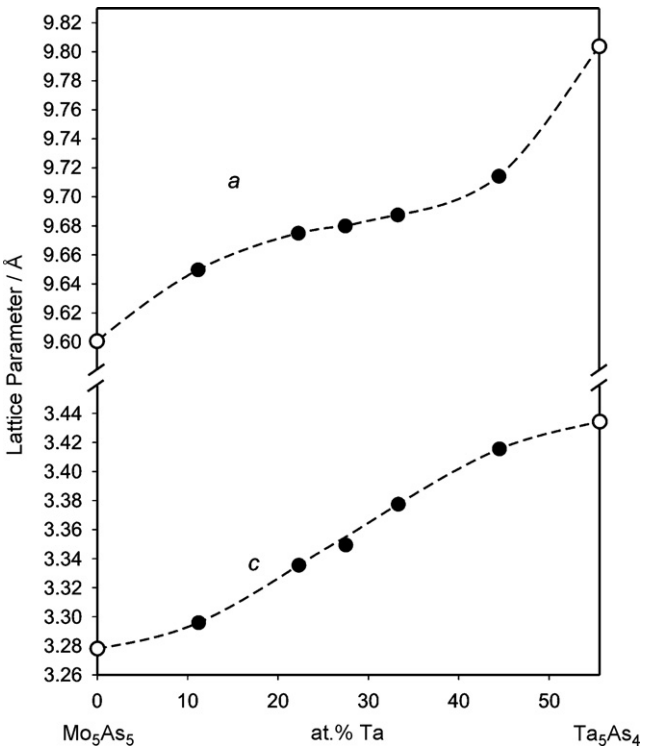

Fig. 2. Lattice parameters of the complete solid solution $(Mo,Ta)_5As_4$ (Ti_5Te_4-type structure) as a function of composition. Black circles: this work; white circles: literature values for binary compounds (Table 1).

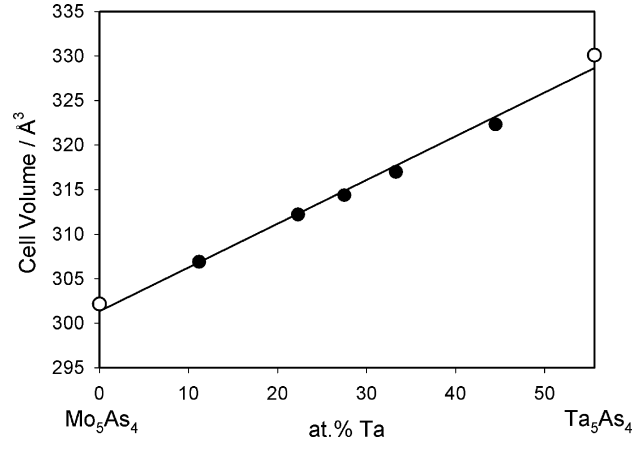

Fig. 3. Cell volume of $(Mo,Ta)_5As_4$ (Ti_5Te_4-type structure) as a function of composition. Black circles: this work; white circles: literature values for binary compounds (Table 1).

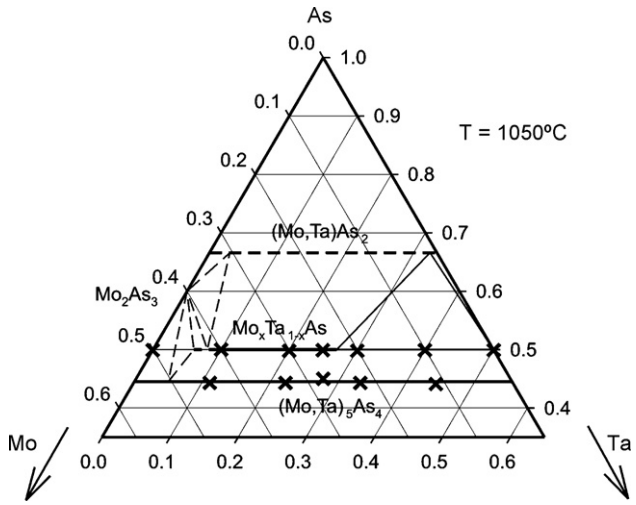

Fig. 4. Arsenic-rich part of the Mo–Ta–As phase diagram at 1050 °C and saturation pressure. Crosses: sample compositions, bold solid lines: intermediate phases; solid lines: tie triangle; bold dashed lines: extrapolated solid solution, dashed lines: extrapolated tie triangles.

refined lattice parameters are not reliable and are consequently not listed separately. The phase fields found by XRD are in agreement with EPMA analysis performed on these samples.

The results of EPMA measurements of the metal-rich samples are summarized in Table 3. Due to significant inhomogenities in different parts of the samples, the phase equilibria observed by EPMA must be considered to be local equilibria and thus the tie-lines and -triangle in some cases do not agree well with the nominal compositions. However, as no experimental data on ternary Mo–Ta–As phase equilibria exist so far, we think it is still worthy to present these data in order to provide a first tentative basis for further studies. In sample #13 the two-phase field of $[(Mo,Ta)+(Mo,Ta)_5As_4]$ was identified by powder XRD, but due to the fine microstructure in this sample only the phase composition of (Mo,Ta) could be measured by EPMA. BSE images showing the microstructures of three different metal-rich samples are given in Fig. 5 and the phase equilibria observed at 1400 °C are given in a partial isothermal section in Fig. 6.

As for 1050 °C, a complete solid solution of Mo_5As_4 and Ta_5As_4 was found at 1400 °C. A significant solubility of Mo in Ta_3As was observed and the solubility limit could be derived from the composition of $Mo_xTa_{3-x}As$ measured in the three phase field $[(Mo,Ta)_5As_4+(Mo_xTa_{3-x}As)+(Mo,Ta)]$ to be around 23 at.% Mo. As the phase Ta_2As was not found in any of the ternary samples, the solubility of Mo in this phase is probably small (in the order of a few at.%). Given the tie line $[(Mo,Ta)_5As_4+(Mo_xTa_{3-x}As)]$ observed in sample #15, it may be concluded that the solubility of Mo in Ta_2As is definitely lower than 18 at.% Mo. For the solid solution (Mo,Ta), the As-content observed in the various ternary samples varied from 0.6 at.% to 3.1 at.%. Given the fine dispersion of (Mo,Ta) in the observed microstructures, we conclude that the lower As-

Table 4
Conditions and results of ternary CVT experiments.

Nominal sample composition at.% Mo/at.% Ta/at.% As	Phase field	[Br]/mg cm^{-3}	[I]/mg cm^{-3}	Phases noticed at the sink
25.1/25.0/49.9	$Mo_xTa_{1-x}As$	0.8	–	–
27.5/27.5/45.0	$(Mo,Ta)_5As_4$	0.8	–	$TaAs_2$
62.7/18.1/19.2	$(Mo,Ta)_5As_4$/(Mo,Ta)	–	1.27	–
35.3/35.3/29.4	$(Mo,Ta)_5As_4/Mo_xTa_{3-x}As$/(Mo,Ta)	0.8	–	β-Ta_2O_5
15.5/53.5/31.0	$(Mo,Ta)_5As_4/Mo_xTa_{3-x}As$	0.8		β-Ta_2O_5
63.2/21.1/15.7	$(Mo,Ta)_5As_4$/(Mo,Ta)	0.8	–	–
42.5/42.5/15.0	$Mo_xTa_{3-x}As$/(Mo,Ta)	0.4	0.6	β-Ta_2O_5
20.6/61.8/17.6	$Mo_xTa_{3-x}As$/(Mo,Ta)	0.8	–	β-Ta_2O_5

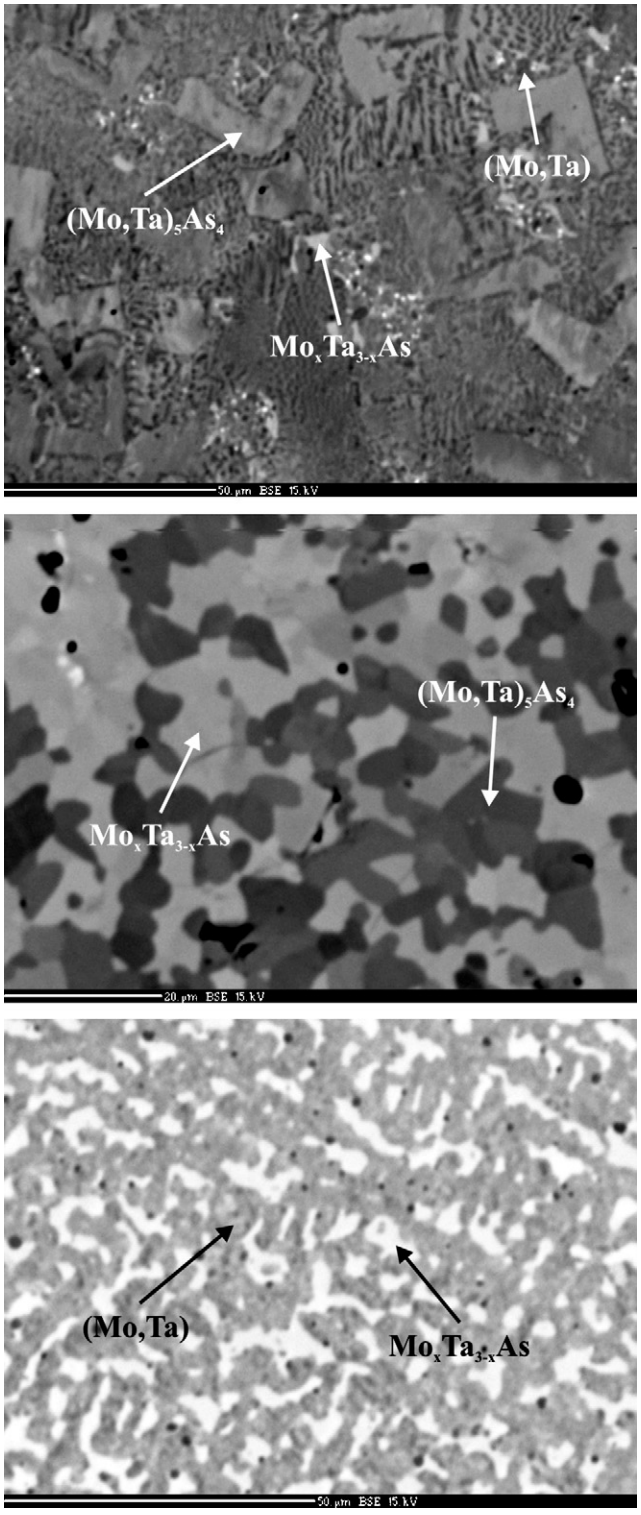

Fig. 5. BSE images showing the microstructures of samples #14 (top), #15 (center) and #17 (bottom) annealed at 1400 °C.

contents are probably the more correct and the higher values stem from neighboring arsenide phases that were obviously measured along with to some extent.

3.3. Chemical vapor transport experiments

In all, eight ternary CVT experiments were performed using two of the As-rich samples (#4 and #10) and all metal-rich samples

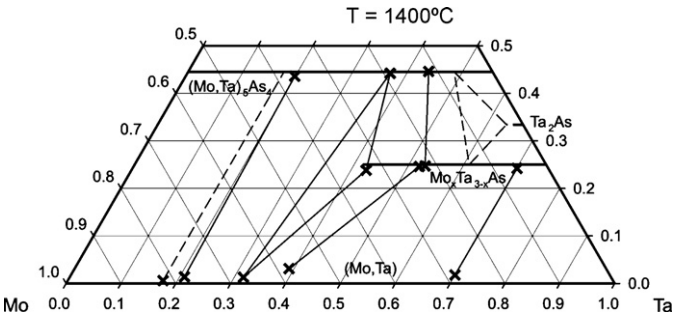

Fig. 6. Metal-rich part of the Mo–Ta–As phase diagram at 1400 °C and saturation pressure. Crosses: compositions determined by EPMA, bold solid lines: intermediate phases; solid lines: tie-lines and -triangle; bold dashed line: extrapolated solid solution, dashed lines: extrapolated tie-line and -triangle.

as source loads. The results of CVT experiments are summarized in Table 4. The concentrations of the transport agent, Br and I, denoted by [Br] and [I], are referred to the volume of the quartz glass tubes, which was 25 cm^3.

Single crystals of arsenides could only be obtained from the transport having $(Mo,Ta)_5As_4$ as charge. These crystals were analyzed by single crystal diffraction and found to be $TaAs_2$. The observed lattice parameters (a = 9.3360(19) Å, b = 3.3840(7) Å, c = 7.7600(16) Å) show that no significant amount of Mo is substituted for Ta in those crystals.

In all experiments where the charge contained $Mo_xTa_{3-x}As$, decomposition of the quartz glass tubes occurred and crystals of β-Ta_2O_5 were observed at the sink. Because the quality of the crystals was too poor for single crystal XRD, powder XRD was performed to identify the phase. The observed powder pattern is in excellent agreement with the pattern reported by Terao [21] for β-Ta_2O_5 which was formed by heating in air. Just as in the current work, Terao was not able to determine the unit cell of this phase, so the crystal structure of β-Ta_2O_5 remains unsolved.

In the CVT experiment with $Mo_xTa_{1-x}As$ as charge no crystal growth was observed at all. The same is true for the two experiments with sources in the two-phase field [$(Mo,Ta)_5As_4$ + (Mo,Ta)], i.e., with the sources showing the highest Mo-content and consequently the lowest activity of Ta in the source.

The results of CVT experiments may be summarized as follows. We did not find evidence for the transport of Mo in any of the experiments as the sinks consisted either of binary $TaAs_2$ or of β-Ta_2O_5 formed by the reaction of Ta-rich crystals with the quartz glass. As binary molybdenum arsenides can be transported using similar conditions (see discussion of literature, chapter 1), we have to conclude that the transport of Mo is suppressed by the presence of Ta due to a shift in the corresponding transport equilibria. However, due to a lack of thermodynamic data for the corresponding solid compounds (in particular no information on the ternary compounds which were reported here for the first time), it is not possible to discuss this point in a thermodynamic context.

Acknowledgements

Financial support from the Austrian Science Foundation (FWF) under the project number P16946-N11 is gratefully acknowledged. The authors also wish to thank Marcus Schmidt for his help with the transport experiments. PR thanks the Max-Planck Gesellschaft for a research fellowship.

References

[1] J.B. Taylor, L.D. Chalvert, M.R. Hunt, Can. J. Chem. 43 (1965) 3045–3051.
[2] P. Jensen, A. Kjekshus, T. Skansen, Acta Chem. Scand. 20 (1966) 403–416.
[3] P. Jensen, A. Kjekshus, Acta Chem. Scand. 20 (1966) 1309–1313.

[4] L.H. Dietrich, W. Jeitschko, J. Solid State Chem. 63 (1986) 377–385.
[5] A. Brown, Nature 206 (1965) 502–503.
[6] H. Boller, H. Nowotny, Chem. Monthly 95 (1964) 1272–1282.
[7] R. Guerin, M. Sergent, J. Prigent, C. R. Acad. Sci. 274C (1972) 1278–1281.
[8] L. Brewer, R.H. Lamoreaux, Bull. Alloy Phase Diag. 1 (1980) 76–78.
[9] J.J. Murray, J.B. Taylor, L. Ulsner, J. Cryst. Growth 15 (1972) 231–239.
[10] S. Furuseth, K. Selte, A. Kjekshus, Acta Chem. Scand. 19 (1965) 95–106.
[11] S. Furuseth, A. Kjekshus, Acta Cryst. 18 (1965) 320–324.
[12] R.G. Ling, C. Belin, C. R. Acad. Sci., Series 2 292 (1981) 891–893.
[13] L.D. Calvert, Acta Cryst. B 48 (1) (1992) 113–114.
[14] J.J. Murray, J.B. Taylor, L.D. Calvert, Y. Wang, E.J. Gabe, J.G. Despault, J. Less-Common Met. 46 (1976) 311–320.
[15] S. Rundqvist, B. Carlsson, C.-O. Pontchour, Acta Chem. Scand. 23 (1969) 2188–2190.
[16] E. Ganglberger, H. Nowotny, F. Benesovsky, Chem. Monthly 97 (1966) 1696–1697.
[17] Y. Wang, L.D. Chalvert, E.J. Gabe, J.B. Taylor, Acta Cryst. B 35 (1979) 1447–1450.
[18] G. Dittmer, U. Niemann, Philips J. Res. 40 (1985) 55–71.
[19] H. Schäfer, J. Less-Common Met. 30 (1973) 141–143.
[20] TOPAS, Bruker AXS Inc., Karlsruhe, Germany, 1999.
[21] N. Terao, Jpn. J. Appl. Phys. 6 (1967) 21–34.